ORIGINAL RESEARCH PAPER
Volume - 12 | Issue - 06 | June - 2023 | PRINT ISSN No. 2277 - 8179 | DOI : 10.36106/ijsr
INTERNATIONAL JOURNAL OF SCIENTIFIC RESEARCH

GRADING BRAIN TUMORS USING ADVANCED MAGNETIC RESONANCE IMAGING SEQUENCES

Radiology

Dr. Harish K* Associate Professor, Dept. of Radio-diagnosis, Shridevi Institute of Medical Sciences & Research Hospital, Tumkur - 572106, Karnataka, India *Corresponding Author

Dr. Divya J Assistant Professor, Dept. of Radio-diagnosis, Shridevi Institute of Medical Sciences & Research Hospital, Tumkur - 572106, Karnataka, India

Dr. Saulam Jacqueline Junior Resident, Dept. of Radio-diagnosis, Shridevi Institute of Medical Sciences & Research Hospital, Tumkur - 572106, Karnataka, India.

Dr. B Vamsi Krishna Reddy Senior Resident, Dept. of Radio-diagnosis, Shridevi Institute of Medical Sciences & Research Hospital, Tumkur - 572106, Karnataka, India.

ABSTRACT

Background: Conventional MR imaging techniques and a variety of advanced techniques have a role in clinical practice or are the subject of research. This study aimed to advance MRI sequences: perfusion, DTI, and spectroscopy and to evaluate the role of advanced MRI sequences for grading intra-axial and extra-axial brain tumors. **Methods:** A hospital-based retrospective observational study of 30 patients was conducted in Tumkur, Karnataka, India. Conventional T1, T2, FLAIR, DWI & ADC, and SWI sequences were used. The advanced MRI imaging techniques perfusion study, spectroscopy, and diffuse tensor imaging were used. To compare the conventional MR imaging parameters based on the tumor grades we performed a Chi-square test. We also conducted Fisher exact test when the assumptions of the Chi-square test were violated. **Results:** The mean age of the patients was 42.5 years. Most of the patients had tumors found in the brain's supratentorial region compared to the infratentorial region (86.7% vs. 13.3%). About 60% of the patients were diagnosed with high-grade tumors. Among our studied patients, all the high-grade brain tumors were detected in patients over 30 years of age whereas half of the patients diagnosed with low-grade tumors were 15 to 30 years of age. Males were found to have higher high-grade tumors compared to females (58.3% vs. 44.4%). Both high and low-grade tumors were found higher in the supratentorial regions of the brain. The mean value of relative cerebral blood volume (rCBV) was found significantly higher in high-grade tumors as compared to low-grade tumors (4.45 vs. 0.62). **Conclusion:** This study has demonstrated the utility of advanced MRI imaging can effectively differentiate different grades of brain tumors.

KEYWORDS

Diffuse tensor imaging (FA fractional anisotropy), MRI perfusion, MR spectroscopy, relative cerebral blood volume (rCBV), high-grade gliomas, low-grade gliomas.

INTRODUCTION

Intracranial tumors form a significant health issue. The annual incidence of primary and secondary central nervous system neoplasms was 19/100000 person-years (8.3/100000 for neuroepithelial tumors and 7.3/100000 for meningeal tumors). [1]

Magnetic resonance imaging (MRI) provides an excellent soft tissue contrast, and the sequence range explores the differences in the brain and tumors' biophysical properties, which made MRI the choice of imaging for brain tumor assessment. Even though MRI has improved tumor visualization, conventional imaging fails to provide adequate information in a few areas such as its inability to show tumor infiltration, being deficient in tumor grading, often insensitive in detecting subtle changes due to treatment effects in tumors, and poor identification of the relationship of white matter or eloquent cortex tracts to tumors.[2]

Therefore, because of these limitations of conventional imaging, advanced MRI has been developed to study biological and pathological changes within tumors. The current advanced techniques include perfusion imaging, diffusion-weighted imaging (including diffusion-tensor imaging), MR spectroscopy, blood oxygen level–dependent (BOLD) imaging, and the largely experimental molecular imaging. [3] In the present study, advanced MRI sequences such as diffusion tensor imaging (DTI), Perfusion MRI, and MR spectroscopy (MRS) were used.

Advanced MR Imaging

Perfusion Imaging:

There are three main methods to study brain perfusion. First, dynamic susceptibility contrast imaging (DSCI), is the most common method and is like to be a standard sequence on most MR machines. Secondly, dynamic contrast enhancement (DCE), that measures changes in the intensity of signal as a bolus of gadolinium diffuses across the damaged blood-brain barrier into the extracellular, extravascular space (EES) by using rapid T1 sequence. And lastly, arterial spin labeling (ASL), is the latest technique largely based on research providing the truly quantitative value of cerebral blood flow. It uses an endogenous contrast mechanism, where blood flow in the brain is magnetically labeled. The advantage of this method is that it can be repeated over a short time frame and can label individual vessels showing their involvement in blood flow into the region.[2]

MR Spectroscopy (MRS):

Magnetic Resonance (MR) spectroscopy is based on the principle of chemical shift.[2] It is a noninvasive test to measure biochemical changes happening in the brain, especially the tumor presence. Normal brain tissue is compared with abnormal tumor tissue by chemical composition. We commonly use hydrogen or proton spectroscopy. To differentiate between tumors, there are various metabolites or metabolism products.[4]

Diffusion tensor imaging (DTI):

In tumors, diffusion anisotropy is reduced due to disruption of normal brain architecture along with loss of tissue organization, widening of extracellular space, destruction of axonal processes, and cell size changes. Cell density [5,6] and proliferation index of glioma [5] are correlated with a reduction in fractional anisotropy. One of the major roles of DTI is to study the tumor effects it has on surrounding white matter tracts.[7]

With the abovementioned three advanced MRI sequences, the present study aimed to evaluate the role of these MRI sequences for grading intra-axial and extra-axial brain tumors.

Methodology

Study population:

It was a hospital-based retrospective observational study conducted over a period of 12 months from September 2021- August 2022 in the Department of Radio-diagnosis of Shridevi Institute of Medical Sciences and Research Hospital, Tumkur, Karnataka, India.

After obtaining approval and clearance from the institutional ethical committee, the patients fulfilling the inclusion criteria were enrolled for the study. We excluded patients who did not meet the inclusion criteria and had any of the features of the exclusion criteria. The patients were referred for neuroimaging to our department from our research hospital and outside of the hospital. For this study, we

included 30 patients diagnosed with a brain tumor during our study window period.

Inclusion criteria:

i. Newly diagnosed brain tumors in our department.
ii. Diagnosed brain tumors either on CT or outside imaging which includes both intra-axial and extra-axial tumors.

Exclusion criteria:

i. The patient refused to give informed consent.
ii. Patients having claustrophobia.
iii. If all sequences could not be done due to the non-cooperation of the patient.
iv. Post-operative brain tumor patients.
v. Brain metastasis.

MRI Process

After appropriate preparation and normal creatinine levels, the patients were subjected to conventional and advanced MRI imaging techniques using a 3Tesla machine (GE Signa). Conventional T1, T2, FLAIR, DWI & ADC, and SWI sequences are used. Advanced MRI imaging techniques: perfusion study, spectroscopy, and diffuse tensor imaging are used.

I. On conventional MRI;

A) Patients were screened for any contraindications to the MRI examination, such as aneurysmal clips or cardiac pacemakers.
B) Sedation was given to irritable patients and pediatrics.
C) The following sequences used in conventional MR examination:

1. Axial, coronal T2-weighted fast spin-echo (T2 TSE) using the following parameters: repetition time (TR) of 8850 ms, echo time (TE) of 170 ms, a slice thickness of 5 mm, a gap of 1 mm, 512 × 512 acquisition matrix, FOV = 260 mm. given an acquisition time of 2 mins.
2. Axial fluid attenuation recovery (FLAIR) using the following parameters: TR of 11000 ms, TE of 140 ms, a slice thickness of 5 mm, a gap of 1 mm, 320 × 320 acquisition matrix, FOV = 260 mm. given an acquisition time of 2 mins 50-secs.
3. Pre- and post-contrast axial and sagittal T1-weighted spin echo (T1 SE) with the following parameters (post-contrast sequences done after perfusion study): TR of 252 ms, a TE of 42 ms, a 320 × 320 acquisition matrix, a field of view (FOV) of 260 mm, a slice thickness of 5 mm, and a gap of 1 mm, given an acquisition time of 2 mins.

II. Advanced neuroimaging

A) MR Spectroscopy

3D multi-voxel CSI with average TE echo time (144 ms) (TR 1000 ms, 15 mm FOV, acquisition time 5 min 30s) to evaluate the levels of choline (Cho) at 3.36– 3.21 ppm, creatinine (Cr) at 3.15–3.0 ppm, and N-acetyl aspartate (NAA) at 2.18–2.01 ppm. The size and position of interest were determined by examining MRI images in three dimensions (sagittal, coronal, and transverse), the goal was to include the largest part of the lesion, the peri-focal region, with the normal contralateral brain region of interest (only with evaluation by multi-voxel 3D CSI) as much as possible and to exclude subcutaneous fat and regions with large variations in magnetic susceptibility. The ratio of metabolites: Cho/Cr and Cho/NAA was calculated by dividing the integral values of the metabolite in the same spectrum and this was done automatically by the station software working.

B) Perfusion-weighted images

1. DSC perfusion sequence:

I We used the dynamic T2 *-weighted gradient echo EPI sequence (TR 850, TE 23-30, matrix 128 x128, slice thickness 8 mm, interval 0.5 mm, number of scans 40acquisitions, and bandwidth 250) during the first pass of a bolus contrast injection.
ii. Perfusion imaging slices should have the same thickness, position, and interval as the FLAIR or T2 axial sequences to facilitate a direct comparison of perfusion results with other pre-contrast sequences.
iii. The phase encoding direction needs to be AP to reduce susceptibility artifacts.
iv. A time series of fast T2-weighted images acquired when gadolinium passes through the tissues, producing a reduction in T2 intensity as a function of local concentration.
v. Six sections were obtained with no gap to cover the whole lesion which was identified on the T2-weighted images. A series of 40 multi-session acquisitions were acquired. The total acquisition time was 1 min 10 s. The first six acquisitions were made before the injection of the contrast agent to establish a baseline before the contrast. At the seventh acquisition, 0.2 mmol/kg bodyweight of gadolinium was injected using a power injector at a flow rate of 5 ml/s through an 18- or 20-gauge intravenous catheter, immediately followed by an injection of a bolus of saline solution at the same rate for a total of 15-20 ml.

2. Post-processing:

All data were transferred to a Adw 4.6 work station and SD version 25 software is used. Spatial and temporal smoothing is applied at a medium degree for improvement of the resolution and reduction of the effect of the motion artifact. We chose the variable gamma adjustment, then the arterial input function, and put a region of interest (ROI) on one of the middle cerebral arteries. Several curves appeared on the left, and then we chose at least five curves almost typical of the normal brain curve and then proceeded. Cerebral blood volume (CBV) color maps were obtained. The maximum regional CBV is calculated by placing the ROI on the area of interest in the solid area with the greatest intensity of color. The ROI is established intratumorally to measure CBV value. These ROIs are drawn on hot spot areas, that is, most hypervascular areas, as shown on the CBV color map. Only the ROI revealed the maximum value for each parameter selected to represent the intratumorally CBVs (CBVt). These ROIs should not include any intratumor vessel, hemorrhagic spot, calcification, or necrosis. Another ROI was drawn in the contralateral normal white matter at the same level. Then, the relative ratios (rCBVt) were calculated by dividing the maximum value of the intratumor region by the value of the contralateral normal white matter and expressed as a ratio of rCBV [ratio = CBV (lesion) / CBV (contralateral normal white matter).

C) Diffuse Tensor imaging

All images were obtained with a 3 T whole-body scanner (GE Signa) with a 16-channel head coil utilizing the sense parallel imaging technique. DTI was acquired by using single-shot spin-echo echo-planar imaging (TR = 8000 ms; TE = 90 ms; bandwidth = 250 Hz; matrix, 128 x 128; FOV 24 mm; slice thickness 4 mm, no gap; b factor = 0 and1,000 mm2/s; directions of gradient sampling, 25). The associated brain mapping MRI protocols were obtained that included axial T2-wi, FLAIR, and post-gadolinium axial T1-wi. The routine cMRI was also obtained including pre-gadolinium sagittal T1-wi, axial and coronal T2-wi, axial FLAIR, axial DWI/ADC map, axial SWI, and post-gadolinium axial, sagittal and coronal T1-WI. Post-processing analysis was performed on commercial software measuring FA and apparent diffusion coefficient (ADC) values by manually placing a region of interest (ROI) within enhancing region of the tumor that represents a high-grade portion or solid non-enhancing region if tumors did not enhance. The measured FA and ADC values within the necrotic region, peritumoral edema, contralateral normal-appearing white matter (NAWM), and normal corpus callosum were also obtained. Each reviewer placed five ROIs in the solid tumoral region, necrotic region, and peritumoral edema to obtain the minimum and maximum FA and ADC values (fewer ROIs for smaller lesions). The average FA and ADC in each area were calculated. The five ROIs were placed in NAWM as well as a single ROI in genu or splenium of corpus callosum and then average FA and ADC values were calculated. The NAWM and corpus callosum were selected as internal normal control and FA and ADC ratios of each lesioned region were calculated.

Statistical analysis

The basic characteristics of the patients with brain tumors were reported as descriptive statistics, presented as percentages. We performed a Chi-square test to compare the conventional MR imaging parameters based on the tumor grades. We also conducted Fisher exact test when the assumptions of the Chi-square test were violated. Moreover, we performed the t-test to assess the differences in advanced MR imaging parameters based on the tumor grades. A P-value of less than 0.05 will be considered significant for all the statistical analyses. We used SPSS (Version 28.0.1, IBM Corporation, Armonk, NY, United States), and GraphPad Prism (Version 9.4.0, GraphPad Software Inc., California, United States), software packages for these analyses.

RESULTS

Table 1: Characteristics of the patients diagnosed with brain tumors (n=30)

Characteristics	n (%)
Age	
15-30 years	9 (30.0)
30-50 years	11 (36.7)
Over 50 years	10 (33.3)
Gender	
Male	15 (50.0)
Female	15 (50.0)
Lobe involved	
Bilateral	1 (3.3)
Left lobe	12 (40.0)
Right lobe	14 (46.7)
Pons and medulla	3 (10.0)
Area involved	
Supratentorial	26 (86.7)
Infratentorial	4 (13.3)
Tumor grade	
High-grade	12 (40.0)
Low-grade	18 (60.0)

Table 1 shows the basic characteristics of the patients diagnosed with brain tumors. There was a similar distribution of patients across the age range with a mean age of 42.5 years. About 37% of the patients were 30 to 50 years of age. Our study diagnosed an equal number of males and females with brain tumors. Most of the patients had tumors found in the brain's supratentorial region compared to the infratentorial region (86.7% vs. 13.3%). About 60% of the patients were diagnosed with high-grade tumors. The distribution of the basic characteristics of the patients based on the grade of tumors is presented in Figure 1. Among our studied patients, all the high-grade brain tumors were detected in patients over 30 years of age whereas half of the patients diagnosed with low-grade tumors were 15 to 30 years of age. The distributions of the high-grade and low-grade tumors across the gender were not found significantly different. However, males were found to have higher high-grade tumors compared to females (58.3% vs. 44.4%). Both high-grade and low-grade tumors were found higher in the supratentorial regions of the brain.

Table 2: Conventional MR imaging parameters based on the tumor grades

	Grades of tumors		Total	p-value
	High grade	Low grade		
	n=12	n=18	n=30	
T1-weighted imaging				0.04
Heterogeneously hypointense	12 (100)	11 (61.1)	23 (76.7)	
Hypointense	0 (0.0)	3 (16.7)	3 (10.0)	
Isointense	0 (0.0)	4 (22.2)	4 (13.3)	
T2-weighted imaging				0.13
Heterogeneously hyperintense	12 (100)	15 (83.3)	27 (90.0)	
Hyperintense	0 (0.0)	3 (16.7)	3 (10.0)	
FLAIR imaging				0.40
Heterogeneously hyperintense	12 (100)	17 (94.4)	29 (96.7)	
Hyperintense	0 (0.0)	1 (5.6)	1(3.3)	
Diffusion restriction				< 0.001
Absent	3 (25.0)	18 (100)	21 (70.0)	
Patchy diffusion	9 (75.0)	0 (0.0)	9 (30.0)	
SWI imaging				< 0.001
Blooming	6 (50.0)	0 (0.0)	6 (20.0)	
No blooming	6 (50.0)	18 (100)	24 (80.0)	

Values are given as, numbers (percentage); n (%)

Table 2 shows the distribution of conventional MR imaging parameters responses based on the tumor grades. All the high-grade tumors in the brain showed heterogeneously hypointense signals in the T1-weighted imaging and heterogeneously hyperintense signals in the T2-weighted and FLAIR imaging. About 61% of the low-grade brain tumors showed heterogeneously hypointense signals in the T1-weighted imaging. In T2-weighted and FLAIR imaging respectively 83% and 94% of the tumors showed hyperintensity heterogeneously. Diffusion restriction was absent in all of the low-grade brain tumors of the patients. No blooming artifact was observed in the low-grade brain tumors, however, about half of the high-grade tumors showed blooming artifacts in the SWI imaging.

Table 3: Advanced neuroimaging parameters based on the tumor grades

	Grades of tumors		Total	p-value
	High grade	Low grade		
	(n=12)	(n=18)	(n=30)	
rCBV	4.45 ± 1.04	0.62 ± 0.20	2.15 ± 2.02	< 0.001
FA	0.17 ± 0.01	0.11 ± 0.01	0.13 ± 0.03	0.240
Cho/Cr	5.71 ± 1.51	1.66 ± 0.09	3.28 ± 2.22	< 0.001
Cho/NAA	5.93 ± 1.05	1.27 ± 0.13	3.13 ± 2.41	< 0.001

Values are given as, mean ± SD; rCBV stands for relative cerebral blood volume; FA stands for Fractional anisotropy Cho/Cr stands for choline and creatine ratio; Cho/NAA stands for choline and N-acetyl aspartate ratio.

Table 3 shows the comparative values of the advanced neuroimaging parameters based on tumor grades. The mean value of relative cerebral blood volume (rCBV) was found significantly higher in high-grade tumors as compared to low-grade tumors (4.45 vs. 0.62). The directionality of molecular displacements by diffusion (fractional anisotropy) of the high-grade and low-grade tumors was not found significantly different. The choline to creatine ratio was found to be significantly higher in the high-grade brain tumors than the low-grade tumors (5.71 vs. 1.66). Moreover, the mean choline to N-acetyl aspartate ratio was also found higher in high-grade tumors (5.93) compared to low-grade tumors (1.27).

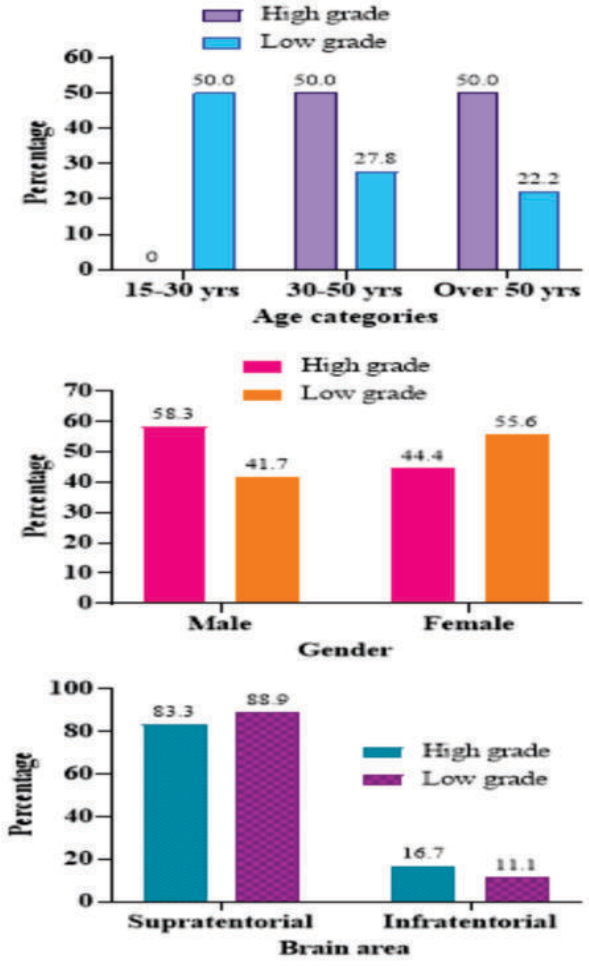

Figure 1: Basic characteristics of the patients based on tumor grades.

DISCUSSION

Conventional MRI constitutes the most used MRI technique in the assessment of primary brain tumors. However, higher accuracy is necessary when grading brain tumors [8]. Few attempts have been made to combine different MRI techniques in grading tumors [8] and, a study by Yoon *et al*. [9] has combined conventional MRI with PWI, DWI, and MRS in a group of patients diagnosed with cerebral gliomas like the present study. That study showed that there were no significant differences in the diagnostic performances of any of those MR imaging techniques.

Results of several studies indicate that rCBV measurements may improve the grading of gliomas. A study by Aronen *et al*. [10] reported mean maximal rCBV values of 3.64 and 1.11 in high- and low-grade gliomas, respectively (n=19). Knopp et al. [11] had almost similar mean maximal rCBV values of 5.07 and 1.44 in high- and low-grade gliomas, respectively (n=29). These study values are comparable to our reporting, with mean maximal rCBV values of 4.45 and 0.62 for high and low-grade gliomas, respectively (Table 3, n=30).

Advanced MR imaging is a useful adjunct to conventional MR imaging in planning, antiangiogenic therapy, postoperative chemotherapy, and radiation therapy. Since these techniques prevent some of the sampling error problems related to histopathologic examination, it is likely that such methods may provide a more accurate overall tumor assessment. [12]

CONCLUSION

The use of advanced MRI imaging can effectively differentiate different grades of brain tumors. The advanced MRI imaging methods perfusion study, spectroscopy, and diffuse tensor imaging have significant correlation with the degree of malignancy, thus predicting different grades of tumors compared to conventional MRI imaging alone, aiding in management and follow-up. So, the utility of advanced MRI imaging sequences in brain tumor imaging provides significant insight regarding the malignancy of the tumor apart from conventional imaging. These are non-invasive techniques and are easily available to help in the prognostication of patients and thus avoiding unnecessary stereotactic biopsies for low-grade gliomas which require follow-up. The utility of advanced MRI imaging sequences in brain tumors for differentiating different grades of tumors forms an integral part of patient management.

REFERENCES

[1] Pouchieu, C., Gruber, A., Berteaud, E., Ménégon, P., Monteil, P., Huchet, A., Vignes, J.-R., Vital, A., Loiseau, H., & Baldi, I. (2018). Increasing incidence of central nervous system (CNS) tumors (2000–2012): findings from a population based registry in Gironde (France). BMC Cancer, 18(1). https://doi.org/10.1186/s12885-018-4545-9

[2] Price, S. J. (2007). The role of advanced MR imaging in understanding brain tumour pathology. British Journal of Neurosurgery, 21(6), 562–575. https://doi. org/10.1080/02688690701700935

[3] Al-Okaili, R. N., Krejza, J., Wang, S., Woo, J. H., & Melhem, E. R. (2006). Advanced MR Imaging Techniques in the Diagnosis of Intraaxial Brain Tumors in Adults. RadioGraphics, 26(suppl_1), S173–S189. https://doi.org/10.1148/rg.26si065513

[4] MRI (magnetic resonance imaging). (n.d.). Www.mayfieldclinic.com. https://mayfieldclinic.com/pe-mrspectroscopy.htm

[5] Beppu, T., Inoue, T., Shibata, Y., Yamada, N., Kurose, A., Ogasawara, K., Ogawa, A., & Kabasawa, H. (2005). Fractional anisotropy value by diffusion tensor magnetic resonance imaging as a predictor of cell density and proliferation activity of glioblastomas. Surgical Neurology, 63(1), 56–61. https://doi.org/10. 1016/j. surneu. 2004.02.034

[6] Stadlbauer, A., Ganslandt, O., Buslei, R., Hammen, T., Gruber, S., Moser, E., Buchfelder, M., Salomonowitz, E., & Nimsky, C. (2006). Gliomas: Histopathologic Evaluation of Changes in Directionality and Magnitude of Water Diffusion at Diffusion-Tensor MR Imaging. Radiology, 240(3), 803–810. https://doi.org/10. 1148/radiol. 2403050937

[7] Witwer, B. P., Moftakhar, R., Hasan, K. M., Deshmukh, P., Haughton, V., Field, A., Arfanakis, K., Noyes, J., Moritz, C. H., Meyerand, M. E., Rowley, H. A., Alexander, A. L., & Badie, B. (2002). Diffusion-tensor imaging of white matter tracts in patients with cerebral neoplasm. Journal of Neurosurgery, 97(3), 568–575. https://doi.org/10.3171/jns.2002.97.3.0568

[8] Guzmán-De-Villoria, J. A., Mateos-Pérez, J. M., Fernández-García, P., Castro, E., & Desco, M. (2014). Added value of advanced over conventional magnetic resonance imaging in grading gliomas and other primary brain tumors. Cancer Imaging, 14(1). https://doi.org/10.1186/s40644-014-0035-8

[9] Yoon, J. H., Kim, J., Kang, W. J., Sohn, C.-H., Choi, S. H., Yun, T. J., Eun, Y., Song, Y. S., & Chang, K.-H. (2013). Grading of Cerebral Glioma with Multiparametric MR Imaging and 18F-FDG-PET: Concordance and Accuracy. European Radiology, 24(2), 380–389. https://doi.org/10.1007/s00330-013-3019-3

[10] Aronen, H. J., Gazit, I. E., Louis, D. N., Buchbinder, B. R., Pardo, F. S., Weisskoff, R. M., Harsh, G. R., Cosgrove, G. R., Halpern, E. F., & Hochberg, F. H. (1994). Cerebral blood volume maps of gliomas: comparison with tumor grade and histologic findings. Radiology, 191(1), 41–51. https://doi.org/10.1148/radiology.191.1.8134596

[11] Knopp, E. A., Cha, S., Johnson, G., Mazumdar, A., Golfinos, J. G., Zagzag, D., Miller, D. C., Kelly, P. J., & Kricheff, I. I. (1999). Glial Neoplasms: Dynamic Contrast-enhanced T2*-weighted MR Imaging. Radiology, 211(3), 791–798. https://doi. org/10.1148/radiology.211.3.r99jn46791

[12] Law, M., Yang, S., Wang, H., Babb, J. S., Johnson, G., Cha, S., Knopp, E. A., & Zagzag, D. (2003). Glioma grading: sensitivity, specificity, and predictive values of perfusion MR imaging and proton MR spectroscopic imaging compared with conventional MR imaging. AJNR. American Journal of Neuroradiology, 24(10), 1989–1998. https://pubmed.ncbi.nlm.nih.gov/14625221/